



INDIAN INSTITUTE OF INFORMATION
TECHNOLOGY AND MANAGEMENT
KERALA
Technopark Campus

An Analytical Comparison of Different Regularization Parameter Selection Methods for Regularization in Auto-Calibrating Parallel MRI

Submitted by
Saradindu Sengupta

Reg. No: 91616006

In partial fulfilment of the requirements for the award of
Master of Science in Computer Science with Specialization in Machine
Intelligence

Conducted by

**INDIAN INSTITUTE OF INFORMATION
TECHNOLOGY AND MANAGEMENT – KERALA**
Technopark Campus,
Thiruvananthapuram, 695-581

April 2017

BONAFIDE CERTIFICATE

This is to certify that the mini project entitled "**An Analytical Comparison of Different Regularization Parameter Selection Methods for Regularization in Auto-Calibrating Parallel MRI**" submitted by **SARADINDU SENGUPTA** in partial fulfillment of the requirement for the award of the **Master of Science in Computer Science with specialization in Machine Intelligence** is a bonafide record of the work under my guidance and supervision at IIITM-K.

Signature of the Supervisor

Dr. Joseph S. Paul
Professor, IIITM-K

Signature of the Course Coordinator

Dr. Asharaf S.
Professor, IIITM-K

Signature of the Head of the Institute

Dr. Rajasree M. S.
Director & Professor, IIITM-K

DECLARATION

I hereby declare that the mini project entitled "**An Analytical Comparison of Different Regularization Parameter Selection Methods for Regularization in Auto-Calibrating Parallel MRI**", submitted in partial fulfillment of the requirements for the ward of degree of **Master of Science in Computer Science with specialization in Machine Intelligence** is substantially the result of my own work except where explicitly indicated in the text carried out during the second semester under the guidance of Dr. Joseph Paul, Associate Professor, IIITM-K. The report may be freely copied and distributed provided the source is acknowledged.

Date : 01.05.2017

Saradindu Sengupta

Place: Thiruvananthapuram

Reg. No: **91616006**

ACKNOWLEDGEMENT

The culmination of my project requires more than one word of thanks to all those who were a part of these efforts that I had undertook for this projection and also in preparing the report.

I am extremely grateful to Dr. Rajasree M S, for providing me with good facilities and a proper environment which helped me in enhancing my ability for undertaking a project of this scale. I thank Dr. Joseph S. Paul, Associate Professor, IIITM-K, Thiruvananthapuram, my guide for his valuable suggestion, appraisal and guidance. I express my heartfelt thanks to Dr. Asharaf S, Assistant Professor, IIITM-K, Thiruvananthapuram, for his valuable support towards the successful completion of my project. I also thank all the teaching and non-teaching staff for their co-operation and support throughout.

I also thank my seniors and all our friends for helping me during various stages of my work. I truly admire my parents for their constant encouragement and enduring support which was inevitable for my success of my ventures and completion of this work.

Saradindu Sengupta

Content	Page No.		
Abstract	6		
1.Introduction	7		
2.Scope of the Study	9		
3.Requirement Specification	3.1.Data sets 3.2.Technical Requirement	10 11	
4.Methods & Materials	4.1Methods 4.2Materials	4.1.1. GRAPPA 4.1.2. SPIRiT 4.2.1. Regularization 4.2.2. Optimum parameter selection Strategies for regularization	12 16 20 21
5.Results	5.1GRAPPA Results 5.2SPIRiT Results	21 22	
6.Discussion		23	
7.Conclusion		23	
Literature Survey		24	
List of symbols		25	
List of Figures & Tables		26	
References		28	

Abstract

This study analyzes the optimality of regularized reconstruction in auto calibrating parallel MRI GRAPPA and SPIRiT. Regularization leads to acceleration in parallel imaging and the selection of regularization factors leads to an optimal reconstruction of the acquired data. This study analytically studies various strategies for obtaining the regularization parameter using L-curve and GCV for spectral cut-off regularization in SPIRiT and GRAPPA image reconstruction for optimal regularization. Performance variations due to adaptation of different methodologies are evaluated. In this study only spectral cut-off regularization has been studied using generalized cross validation and L-curve as regularization parameter selector. All the experiments have been performed on seven set of volunteer data sets procured through Siemens 1.5T Magnetom-Avanto clinical MR scanner. The experiment results show that presence of sharp L-corner does not guarantee in artifact free image; For same no of ACS lines and sampling factor sharp L-corners are better observed in SPIRiT compared to GRAPPA reconstruction; parameter values based on GCV always exceeds of that L-curve. Minimization in noise propagation during reconstruction phase and diminishing the effect of aliasing can be achieved with the effective use of regularized solution.

Keywords: GRAPPA, SPIRiT, image-reconstruction, parallel-MRI, L-curve, GCV, Regularization-factor, spectral cut-off.

Introduction

Parallel MRI is a robust process of speedy acquisition of MRI data. Parallel imaging is a widely-used technique where the known placement and sensitivities of receiver coils are used to assist spatial localization of the MR signal. Having this additional information about the coils allows reduction in number of phase-encoding steps during image acquisition. This, in turn, potentially results in a several-fold reduction in imaging time. In parallel MR imaging, a reduced data set in the phase encoding direction(s) of k-space is acquired to shorten acquisition time, combining the signal of several coil arrays. The spatial information related to the phased array coil elements is utilized for reducing the amount of conventional Fourier encoding.

First, low-resolution, fully Fourier-encoded reference images are required for sensitivity assessment. Parallel imaging reconstruction in the Cartesian case is efficiently performed by creating one aliased image for each array element using discrete Fourier transformation. The next step then is to create a full FOV (field of view) image from the set of intermediate images. Parallel reconstruction techniques can be used to improve the image quality with increased signal to noise ratio, spatial resolution, reduced artifacts, and the temporal resolution in dynamic MRI scans.

Parallel imaging algorithms can be divided into 2 main groups:

- **Image reconstruction produced by each coil** (reconstruction in the image domain, after Fourier transform): SENSE (Sensitivity Encoding), PILS (Partially Parallel Imaging with Localized Sensitivity), ASSET.
- **Reconstruction of the Fourier plane of images from the frequency signals of each coil** (reconstruction in the frequency domain, before Fourier transform): GRAPPA, SPIRiT.

Additional techniques include SMASH, SPEEDER and mSENSE (an image based enhanced version of SENSE).

The second type of technique is referred as “data driven reconstruction” because they are based on limited knowledge of the underlying physical process and rely on training data to calibrate the relationship between input and output data. Both types of reconstruction require calibration for either coil sensitivity estimation or interpolation coefficients for k-space reconstruction.

- **Non-Parallel MRI vs Parallel MRI**

For example, a set of 4 receiver coils surrounding a head being used to detect the MR signal arising from a pixel. Because each coil is at a different distance from the pixel, the signal recorded by each coil varies as a function of position (closer coils have stronger signals). Just by looking at the relative intensities from each coil, it is possible to make a crude prediction of the approximate source of the MR signal.

In "regular" (non-parallel) imaging, multiple surface coils may be used to detect the MR signal, but their individual outputs are combined into one aggregate complex signal that is digitized and processed into the final image. In parallel imaging, conversely, the signals from individual coils are amplified, digitized, and processed simultaneously "in parallel" along separate channels, retaining their identities until near the end.

Scope of the study

In our study of different regularization methods, both types of reconstruction techniques need calibration to estimate coil sensitivity or interpolation coefficients for k-space reconstruction. It is performed by finding the solution of a system of equations connecting matrix and the corresponding set of observations from each coil.

The two most popular regularized methods are

- Spectral cut off; also, known as Truncated SVD(TSVD)
- Tikhonov Regularization; also, known as weight decay, ridge regression or Wiener filtering

In TSVD method the expansion of the SVD solution is truncated whereas in Tikhonov regularization an extra damping is added to each SVD component of the solution. As performance of the regularization methods depend on the choice of regularization parameter (λ) in both cases in Tikhonov and TSVD methods, a quantitative analysis of the reconstruction performance is required in order to analyze the appropriateness of the standard selection properties for both GRAPPA and SPIRiT reconstruction algorithms.

In this study we, analyze the different strategies for defining optimum regularization parameter in auto-calibrating parallel MRI using both GRAPPA and SPIRiT image reconstruction. Variations arising from various strategies used determining the regularization parameter are evaluated using reconstruction error on basis of number of iterations needed. The methods adopted for determination of regularization parameter are L-curve and GCV. In both cases (i.e. SPIRiT and GRAPPA) both parameter selection techniques are used at under-sampling rate (R) for 2 and 3.

In this study, only one regularization method is quantitatively analyzed, i.e. Truncated SVD, using L-curve and GCV at different under-sampling rate (2,3). The reconstruction error analyzed from the results are then used to determine a viable strategy to choose an optimum regularization parameter.

Requirements Specification

❖ Data sets:

Raw k-space data were acquired from Siemens 1.5T Magnetom-Avanto clinical MR scanner at Sree Chitra Tirunal Institute of Medical Science and Technology, Trivandrum, India. All subjects were volunteers with prior written informed consent collected before scanning. The data consists of fully sampled brain images acquired using array head coil and spine images acquired using surface coils. The data sets used in this study are:

Dataset—I

16-channel brain data acquired using FLAIR sequence (TE = 89ms, TR = 9000ms, Tl: 2500ms, in—plane resolution = 1.0 mm, slice thickness = 5.0 mm FOV = 240 mm).

Dataset-II

6-channel brain data using T₂-weighted spin echo sequence (TE = 92 ms, TR = 4500 ms, in-plane resolution = 1.0 mm, slice thickness = 5.0 mm, FOV = 240 mm).

Dataset—II

32-channel brain data SW1 gradient echo sequence (TE=15ms, TR=349 ms, in- plane resolution = 1.0 mm, slice thickness = 2 mm, F 0V == 230 mm, Hip angle=200).

Dataset-IV

12-channe1 physical phantom T₂ weighted spin echo sequence (TE =10 ms, TR = 200 ms, in-plane resolution = 1.0 mm, slice thickness = 5.0 mm, FOV = 230 mm).

Dataset-V

14-channel spine data acquired using T₂ weighted spin echo sequence (TE = 98 ms, TR = 4500 ms, in-plane resolution = 1.0 mm, slice thickness = 5.0 mm, FOV = 400 mm).

Dataset-VI

4-channe1 spine data using T₂-Weighted spin echo sequence (TE = 98 ms, TR = 3520 ms, in-plane resolution = 1.0 mm, slice thickness = 5.0 mm, FOV = 230 mm).

Dataset-VII

6-channel brain data using FLAIR spin echo sequence (TE = 891113, TR = 9000ms, TI= 2500ms, in-plane resolution=1.0 mm, slice thickness = 5.0 mm, FOV == 240 mm).

❖ Technical Specification:

The experiments were conducted in MATLAB (version 2015a) using openly available templates for experiments in GRAPPA and SPIRiT. The figures (curves and reconstructed images then were saved in MATLAB figure format).

Methods and Materials

❖ Methods:

● Generalized Auto-calibrating Partially Parallel Acquisitions(GRAPPA)

An auto-calibration scan (ACS) can help to improve the reconstructions in k-space based parallel MRI, such as GRAPPA. GRAPPA or Generalized Auto-calibrating Partially Parallel Acquisitions is a parallel imaging technique for fast image acquisition. The frequency domain of image is reconstructed from the frequency signal of each coil. This information is obtained from several k-space lines which are acquired in addition to the normal image acquisition. In self-calibrating parallel magnetic resonance imaging, variable density sampling in k-space is typically employed along the phase encoding(PE) direction, wherein low spatial frequency signals are fully sampled while high spatial frequency signals are under-sampled by an outer reduction factor. Usually ACS is acquired at the center of k-space for higher SNR, thus constituting of full-FOV low-resolution prior images in the channels of an RF coil array Missing signals are reconstructed directly in k-space using the spatial correlation, which is already calculated in the central region of k-space, with their neighboring measured signals. The spatial correlation, also known as the convolution kernel is calculated during calibration, in which multiple measured signals from all coils close to a target signal, and then fit to the corresponding signals in an individual coil k-space.

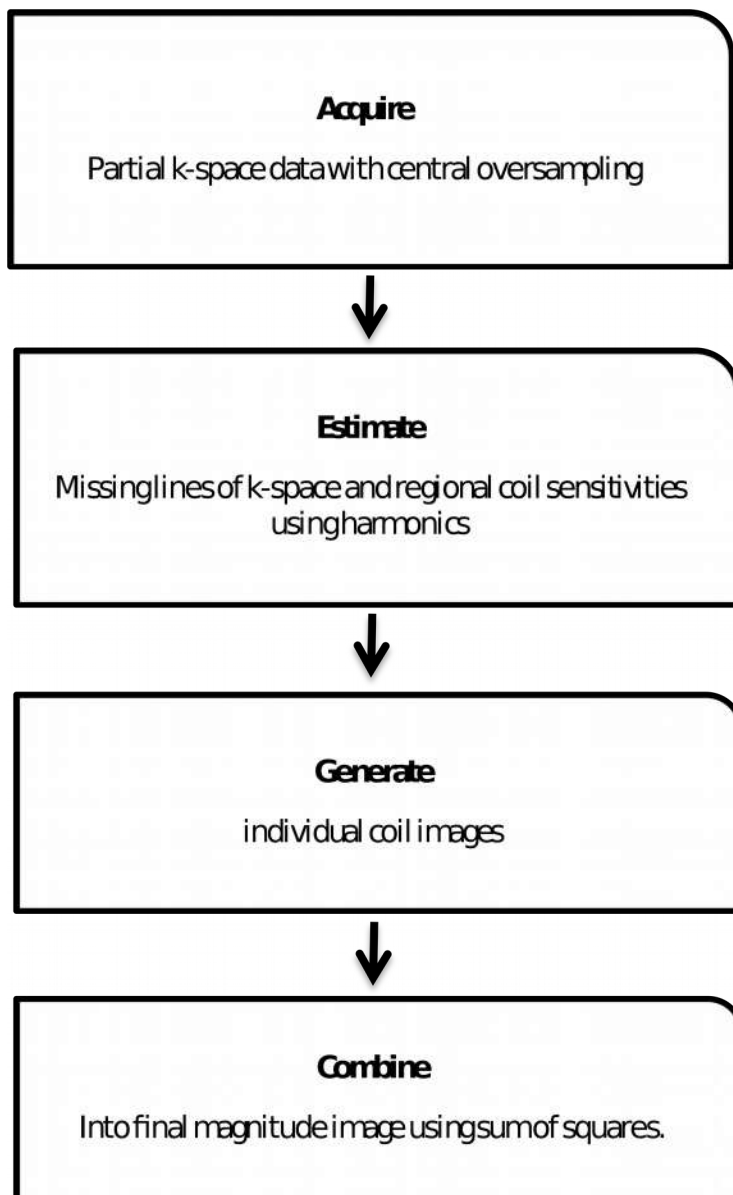


Fig a: - GRAPPA work-flow diagram

Calibration is performed using samples from ACS lines, forming the training data. For acquisition with number of coils = n_c , the weights are dependent on an index $r=1, 2, R-1$, that reflects the distance of an unacquired from its nearest acquired line. Considering k_y to be the PE index of

an acquired line, the basic GRAPPA model can be described as one trying to fit the target data $K^1(k_y + r \Delta k_y, k_x)$ to the nearest source data at location (k_x, k_y) . Hence we can represent this model using the equation

$$K^1(k_y + r \Delta k_y, k_x) = z_r^1 k(k_x, k_y)$$

Where $k(k_x, k_y)$ represents a collection of samples. Let us assume the kernel size is $[a \times b]$,

where a is the number of lines and b is the number of samples of each line included in the kernel.

At first, the calibration weights z_r^l are obtained by inversion of the equation for all training pairs

$\{k(k_y, k_x), K^1(k_y + r \Delta k_y, k_x)\}$ within ACS. k_y refers to only those lines within the ACS that follow the ordering of acquired lines in the under sampled k region. Each point in the ACS lines

contribute to a single row $k(k_x, k_y)$ in the calibration matrix M . The observation vector k_u for calibration is obtained from the formula:

$$z_r^l = (M^H M)^{-1} M^H k_u$$

Following calibration, estimation of a missing k -space value is achieved by applying the filter z_r^l to the nearest acquired dataset $k(k_y, k_x)$. On generalizing the expression for GRAPPA reconstruction, the missing k -space lines in the j^{th} coil is obtained as

$$K^j(k_y + r \Delta k_y, k_x) = \sum_{l=1}^{n_c} \sum_{b=-P_l}^{P_h} \sum_{h=-F_l}^{F_h} K^l(k_y + b R \Delta k_y, k_x + h \Delta k_x) z_r^l$$

Here, b and h are sampling indices of the neighboring points along phase and encoding directions respectively.

Once all of the lines are reconstructed for a particular coil, a Fourier transform can be used to generate the uncombined image for that coil. Once this process is repeated for each coil of the

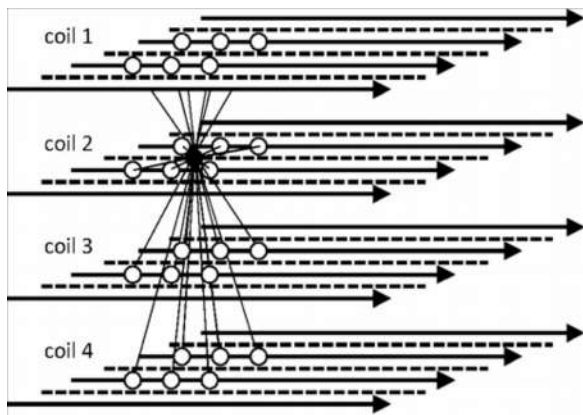


Fig b: - Signal acquisition from different coil

array, the full set of uncombined images can be obtained, which can then be combined using a normal sum of squares reconstruction. By increasing size of the kernel, GRAPPA includes more information into the estimation, thus improving its fit.

Two main categories of error exist with the GRAPPA technique: model error and noise-related error. Model error has two components: one from using a limited number (as well as position) of ACS lines instead of the true coil sensitivity maps and the other from using a limited kernel size. Noise-related error arises from noise in the measured data and includes noise-induced errors that occur during kernel weights estimation, mainly due to the matrix inversion process, and errors that result from the application of the weights to noisy measured data. error. As with any fitting approach, the model error is expected to decrease with increasing kernel size, while the noise-related error is expected to increase with the kernel size. To date, the problem of how to choose a kernel support that optimizes the tradeoff between these errors has not been fully addressed. The choice of the kernel support has been shown to depend on the coil configuration, noise level in the acquired data, imaging field of view and orientation, and number and position of ACS lines. Therefore, GRAPPA implementations employing a fixed kernel support for all situations, as commonly used, are unlikely to be optimal.

- **Iterative Self-Consistent Parallel Imaging Reconstruction (SPIRiT):**

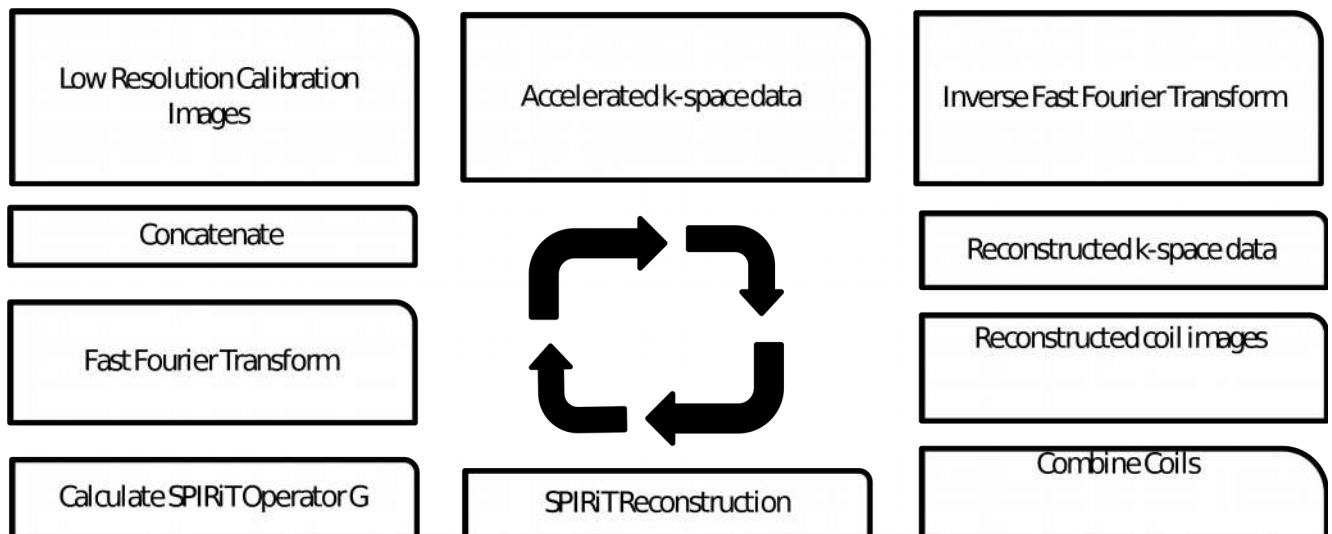


Fig c: - SPIRiT work-flow diagram

The key approach is to separate the consistency constraints into two:

- Consistency with calibration
- Consistency with data acquisition

● **Consistency with calibration**

Let $x_i(r)$ denote an unacquired k-space value at position r , in the i th coil, R_{ir} denote a vector of all points in the neighborhood of $x_i(r)$ on a Cartesian grid and R_{ir}^p denote a subset of R_{ir} containing only acquired points. Consistency is enforced in the grid, i.e., $x_i(r)$, and its entire neighborhood across all coils. It is important to emphasize that the notion, entire neighborhood, includes all the k-space points near $x_i(r)$ in all coils whether they were acquired or not.

Given this the consistency equation for all k-space positions is given by,

$$X_i(r) = \sum_j (g_{ji}, R_{ir})$$

Here g_{ji} is a full kernel independent of the actual k-space sampling pattern and is the same for all k-space positions.

The calibration kernel can be written as

$$X = Gx$$

The matrix G is in fact a series of convolution operators that convolve the entire k-space with the appropriate calibration kernels,

$$X_i = \sum_j (g_{ji}, X_j)$$

Applying the operation G on x is the same as attempting to synthesize every point from its neighborhood. If x is indeed the correct solution, then synthesizing every point from its neighborhood should yield the exact same k-space data.

● Consistency with data acquisition

This constraint can also be expressed as a set of linear equations in matrix form. Let y be the vector of acquired data from all coils (concatenated). Let the operator D be a linear operator that relates the reconstructed Cartesian k-space, x , to the acquired data. The data acquisition consistency is given by

$$Y = Dx$$

This formulation is very general in the sense that x is always Cartesian k-space data, whereas y can be data acquired with arbitrary k-space sampling patterns. In Cartesian acquisitions, the operator D selects only acquired k-space locations. The selection can be arbitrary, uniform, variable density or pseudo random patterns. In non-Cartesian sampling, the operator D represents an interpolation matrix. It interpolates data from a Cartesian k-space grid onto non-Cartesian k-space locations in which the data were acquired.

The steps for non-Cartesian k-space based reconstruction are as follows:

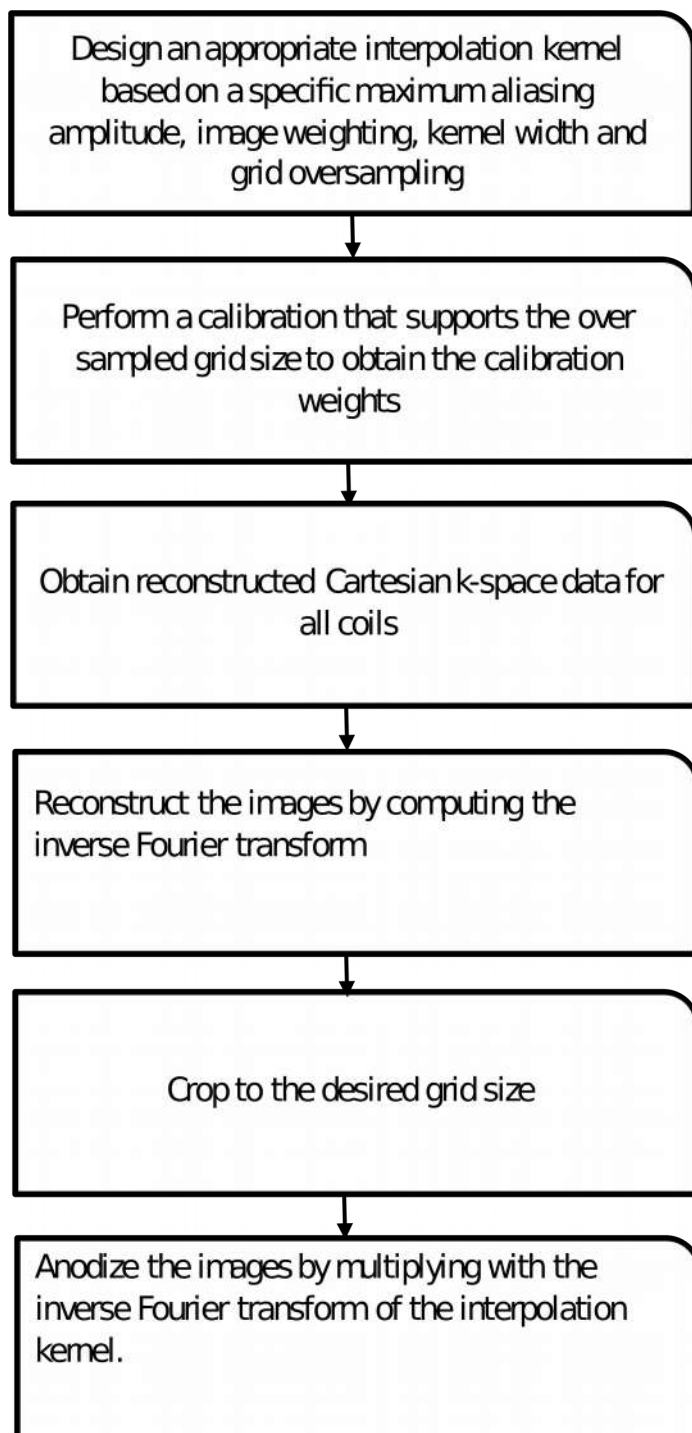


Fig d: - SPIRiT Reconstruction stages

-
- ❖ **Materials:**
 - **Regularization:**

Ill-conditioning causes noise amplification during image reconstruction, which initially limited the application of parallel imaging to only moderate acceleration. This limitation can be overcome by incorporating prior knowledge about the image using regularization methods. In the simplest case, regularization may consist of a basic quadratic penalty in the framework of a linear reconstruction, or make use of much more sophisticated techniques which exploit the structure of images but demand a non-linear reconstruction.

Regularization can be interpreted as prior knowledge and the optimizer as a maximum a posteriori (MAP) estimate of the image. Although regularization leads to a fundamental trade-off between bias and noise - which has to be chosen carefully for optimal image quality - it makes the use of higher acceleration possible. An optimal estimate in terms of mean squared error can only be obtained with regularization. For optimal results, the prior knowledge should include as much specific knowledge about the image as possible. For example, regularization can exploit smoothness in the time domain. Although regularization leads to a fundamental trade-off between bias and noise - which has to be chosen carefully for optimal image quality - it makes the use of higher acceleration possible. An optimal estimate in terms of mean squared error can only be obtained with regularization.

- **Optimum parameter selection Strategies for regularization:**

A regularized estimate \hat{z} is a tradeoff between regularization(bias) and perturbation error(variance). With increase in regularization the regularization error increases and perturbation error decreases.

The optimum parameter selection strategies aim to minimize the sum of bias and variances. Current technique for regularization parameter selection are discrepancy principle, generalized cross-validation and L-curve.

In this study regularized versions of GRAPPA and SPIRiT reconstructions using spectral cutoff regularization (Truncated SVD) are compared using different parameter selection strategies:

- A) L-curve
- B) GCV

A. L-curve method for selection of truncation parameter in Truncated SVD

In TSVD regularization, the L-curve is plotted as a log-log function of residual norm $\|\prod z_k - K_u\|$ versus the solution norm $\|L_{zk}\|$ for varying parameter k. In TSVD the filter factor is 1 if the i^{th} singular value is greater than or equal to the k^{th} singular value and 0 otherwise. Thus TSVD corresponds to a spectral cut-off filter that simply cuts off the last $(n-k)$ components.

B. GCV method for selection of truncation parameter in Truncated SVD

In TSVD, the regularization parameter K is chosen so as to minimize the GCV function

$$G(K) = \frac{\|\prod Z_k - K_u\|_2^2}{T^2}$$

Where $T=n-K$ which is effective number of degrees of freedom

RESULTS

❖ GRAPPA results:

All reconstructions are performed on previously acquired data with acceleration factor 2 and 3 respectively with varying ACS lines depending on the data set [Table-1] by computing optimum kernel size.

Table 1 Here

- **L-curve method for selecting truncation parameter in TSVD:**

Fig-1 and Fig-5 shows the plots of solution norm versus residual norm for data sets I to VII. The circles indicate values of regularization parameter at each point on the L-curve. The optimum parameter is at the corner of the L-curve. Dataset II and III shows sharp L-curve corner. Images reconstructed using parameter chosen from L-curve corner are shown in Fig-2 and Fig-6.

- **GCV method for selecting truncation parameter in TSVD:**

Fig-3 and Fig-7 shows the GCV values plotted as function of the truncation parameter using TSVD regularization. The k -values are indicated by circles and the optimum values are indicated as asterisks (*). The reconstructed images are shown in Fig-4 and Fig-8. The optimum parameter values are higher than in L-curve in some cases.

❖ SPIRiT results:

- **L-curve method for selecting truncation parameter in TSVD:**

Calibration matrix is constructed using both acquired and non-acquired samples within ACS. The resulting L-curves are shown in Fig-9 and Fig-13. The circles indicate values of regularization parameter at each point on the L-curve. Image reconstructed using the parameter values are shown in Fig-10 and Fig-14. The residual aliasing in Data Set V and VI is evident. Data sets II, III, VII shows sharp l-curve. All other data sets show similar performance as GRAPPA.

- **GCV method for selecting truncation parameter in TSVD:**

Fig-11 and Fig-15 shows the GCV values plotted as a function of the truncation parameter. The optimum parameter is indicated using asterisk (*). It is evidently clear that optimum parameter values are higher than L-curve. The reconstructed images are show in Fig-12 and Fig-16. Data set V shows significant amount of aliasing and data set VI shows quiet amount of noise.

Discussions

Selection of appropriate regularization parameter leads to accuracy in regularized outputs. In Parallel MRI, the optimum parameter controls the degree of regularization and thus the compromise in SNR and artifacts. Under-regularization leads to residual noise or artifacts in the image, over regularization removes image features and enhances aliasing. In this study, L-curve and GCV are adopted for optimum parameter selection in spectral cut-off regularization for SPIRiT and GRAPPA.

Only in a subset of the data sets L-curve show sharp corner though an existence of sharp L-corner does not guarantee in artifacts free image construction. Although artifacts always appear where sharp L-curves are not present. With increasing matrix size the L-curve stops behaving consistently leading to over regularization.

Also, GCV shows minimum only in a handful of data sets where in most of the sets GCV is flat with multiple local minima.

Conclusion

As both the reconstruction techniques involves discrete ill-posed least squares noisy reconstruction and artifacts are expected. Though proper and efficient use of regularization and optimal parameter selection can lead to a healthy reconstruction. But the choice of regularization parameter is only reasonable in the presence of a knowledgeable error bound. Without such information a priori, regularization leads to sub-optimal results.

Reconstruction error is much more less in TSVD based on GCV merit function. In all cases L-curve based regularization parameter values are higher than those in GCV though sharp L-curve are not evident throughout the data sets and presence of sharp L-corner does not guarantee in artifact free reconstruction.

For future working scope, the analytically study of Tikhonov regularization for L-curve and GCV based on this study can be a feasible comparison.

Literature Survey

❖ Tikhonov Regularization:

Tikhonov regularization is the most commonly used method of regularization of ill-posed problems. Suppose that for a known matrix A and vector b, we wish to find a vector x such that

$$Ax = b$$

The standard approach is ordinary least squares linear regression. However, if no x satisfies the equation or more than one} x does — that is, the solution is not unique — the problem is said to be ill posed. In such cases, ordinary least squares estimation leads to an overdetermined (over-fitted), or more often an underdetermined (under-fitted) system of equations. Most real-world phenomena have the effect of low-pass filters in the forward direction where A maps x to b. Therefore, in solving the inverse-problem, the inverse mapping operates as a high-pass filter that has the undesirable tendency of amplifying noise (eigenvalues / singular values are largest in the reverse mapping where they were smallest in the forward mapping).

❖ L-Curve:

The L-curve is a log-log plot of the norm of a regularized solution versus the norm of the corresponding residual norm. It is a convenient graphical tool for displaying the trade-off between the size of a regularized solution and its fit to the given data, as the regularization parameter varies. The L-curve thus gives insight into the regularizing properties of the underlying regularization method, and it is an aid in choosing an appropriate regularization parameter for the given data. In this chapter, we summarize the main properties of the L-curve, and demonstrate by examples its usefulness and its limitations both as an analysis tool and as a method for choosing the regularization parameter

❖ Generalized Cross Validation:

Cross-validation, sometimes called rotation estimation, is a model validation technique for assessing how the results of a statistical analysis will generalize to an independent data set.

❖ ASSET & SENSE:

SENSE (*SENSitivity Encoding*) and ASSET (*Array coil Spatial Sensitivity Encoding*) are among the most widely used parallel imaging methods. These techniques are primarily performed in image space after reconstruction of data from the individual coils. (This contrasts with GRAPPA/ARC methods which operate primarily on k-space data before image reconstruction). Each major MR

vendor offers some version of the SENSE technique under different trade names: Siemens (mSENSE), GE (ASSET), Philips (SENSE), Hitachi (RAPID - "Rapid Acquisition through Parallel Imaging Design"), and Toshiba (SPEEDER).

❖ **ACS:**

An auto-calibration scan (ACS) can help to improve the reconstructions in k-space based parallel MRI, such as GRAPPA. Usually ACS is acquired at the center of k-space for higher SNR, thus constituting of full-FOV low-resolution prior images in the channels of an RF coil array.

List of Abbreviations

1. **pMRI** - Parallel Medical Resonance Imaging
2. **SENSE** - SENsitivity Encoding
3. **ASSET** - Array Coil Spatial Sensitivity Encoding
4. **GRAPPA** - Generalized Auto Calibrating Partially Parallel Acquisitions
5. **PILS** -Partially Parallel Imaging with Localized Sensitivity
6. **SPIRiT** - Iterative Self-Consistent Parallel Imaging Reconstruction
7. **ACS** - Auto Calibration Signal / Auto Calibrating Scan
8. **FOV** - Field of View

List of Figures

Fig 1 :- L-Curve for TSVD regularization using GRAPPA with R=2.

Fig. 2: - GRAPPA reconstructed images using TSVD regularization with L-Curve based parameter selection

Fig. 3: - GCV for TSVD regularization using GRAPPA with R=2.

Fig. 4: - GRAPPA reconstructed images using TSVD regularization with GCV based parameter selection.

Fig. 5: -L-Curve for TSVD regularization using GRAPPA with R=3.

Fig 6: - GRAPPA reconstructed images using TSVD regularization with L-Curve based parameter selection.

Fig. 7: - GCV for TSVD regularization using GRAPPA with R=3.

Fig 8: - GRAPPA reconstructed images using TSVD regularization with GCV based parameter selection.

Fig. 9: - L-Curve for TSVD regularization in SPIRiT with $R = 2$

Fig. 10: - SPIRiT reconstructed images using TSVD regularization with L-curve based parameter selection

Fig. 10: - SPIRiT reconstructed images using TSVD regularization with L-curve based parameter selection

Fig. 11: - GCV for TSVD regularization in SPIRiT with $R = 2$

Fig 12: - SPIRiT reconstructed images using TSVD regularization with GCV based parameter selection

Fig. 13: - L-Curve for TSVD regularization in SPIRiT with $R = 3$

Fig. 14: - SPIRiT reconstructed images using TSVD regularization with L-curve based parameter selection

Fig. 15: - GCV for TSVD regularization in SPIRiT with $R = 3$

Fig 16: - SPIRiT reconstructed images using TSVD regularization with GCV based parameter selection

List of Tables

Table 1: - Description of datasets I to VII

Table 2: - Reconstruction error of GRAPPA reconstructed images using TSVD regularization method

Table 3: - Reconstruction error of SPIRiT reconstructed images using TSVD regularization method

Table 4: - Parameters of cross-over determination in GRAPPA calibration for datasets I to VII with $R=2$

Table 5: - Parameters of cross-over determination in GRAPPA calibration for datasets I to VII with $R=3$

Table 6: - Parameters of cross-over determination in SPIRiT calibration for datasets I to VII with $R=2$

Table 7: - Parameters of cross-over determination in SPIRiT calibration for datasets I to VII with $R=3$

Reference

- [1] Michael Lustig, John M. Pauly. SPIRiT: Iterative Self-Consistent Parallel Imaging Reconstruction from Arbitrary k-Space. *Magn Reson Med.* 2010 August; 64(2): 457–471. doi:10.1002/mrm.22428.
- [2] W. Scott Hoge, Dana H. Brooks. Using GRAPPA to improve auto-calibrated coil sensitivity estimation for the SENSE family of parallel imaging reconstruction algorithms. *Magn Reson Med.* 2008 August; 60(2): 462–467. doi:10.1002/mrm.21634.
- [3] Arjun Arunachalam, Alexey Samsonov, Walter F. Block. Self-Calibrated GRAPPA Method for 2D and 3D Radial Data. *Magnetic resonance in Medicine* (2007).
- [4] Anagha Deshmane, MEng, Vikas Gulani, MD, PhD, Mark A. Griswold, PhD, Nicole Seiberlich, PhD. Parallel MR Imaging. *J Magn Reson Imaging.* 2012 July; 36(1): 55–72. doi:10.1002/jmri.23639.
- [5] D. S. Weller, J. R. Polimeni^{2,3}, L. Grady, L. L. Wald^{2,3}, E. Adalsteinsson, V. Goyal. SpRING: Sparse Reconstruction of Images using the Null space method and GRAPPA. *Proc. Intl. Soc. Mag. Reson. Med.* 19 (2011).
- [6] Leslie Ying, Dan Xu, Zhi-Pei Liang. ON TIKHONOV REGULARIZATION FOR IMAGE RECONSTRUCTION IN PARALLEL MRI. Proceeding of the 26th Annual International Conference, IEEE EMBS, 2007.
- [7] Roger Nana, Tiejun Zhao, Keith Heberlein, Stephen M. LaConte, and Xiaoping Hu. Cross-Validation-Based Kernel Support Selection for Improved GRAPPA Reconstruction. *Magnetic resonance in Medicine* (2008).

-
- [9] Peng Qu, PhD, Chunsheng Wang, PhD, and Gary X. Shen, PhD. Discrepancy-Based Adaptive Regularization for GRAPPA Reconstruction. JOURNAL OF MAGNETIC RESONANCE IMAGING 24:248 –255 (2006).
- [10] Daniel S. Weller¹, Sathish Ramani, Jon-Fredrik Nielsen, and Jeffrey A. Fessler. Monte Carlo SURE-Based Parameter Selection for Parallel Magnetic Resonance Imaging Reconstruction. Magn Reson Med. 2014 May; 71(5): 1760–1770. doi:10.1002/mrm.24840.
- [11] Martin Uecker . Parallel Magnetic Resonance Imaging. July2007.
- [12] Chunli Wu,Wenjuan Hu,Ruwen Kan. An improved GRAPPA image reconstruction algorithm for parallel MRI. Control and Decision Conference (CCDC), 2011 Chinese, IEEE Xplore: 01 August 2011.
- [13] Stefan O. Schönberg, Olaf Dietrich, Maximilian F Reiser. Parallel Imaging in Clinical MR Applications. Springer Science & Business Media, 11-Jan-2007
- [14] [University of California, Berkley](#)

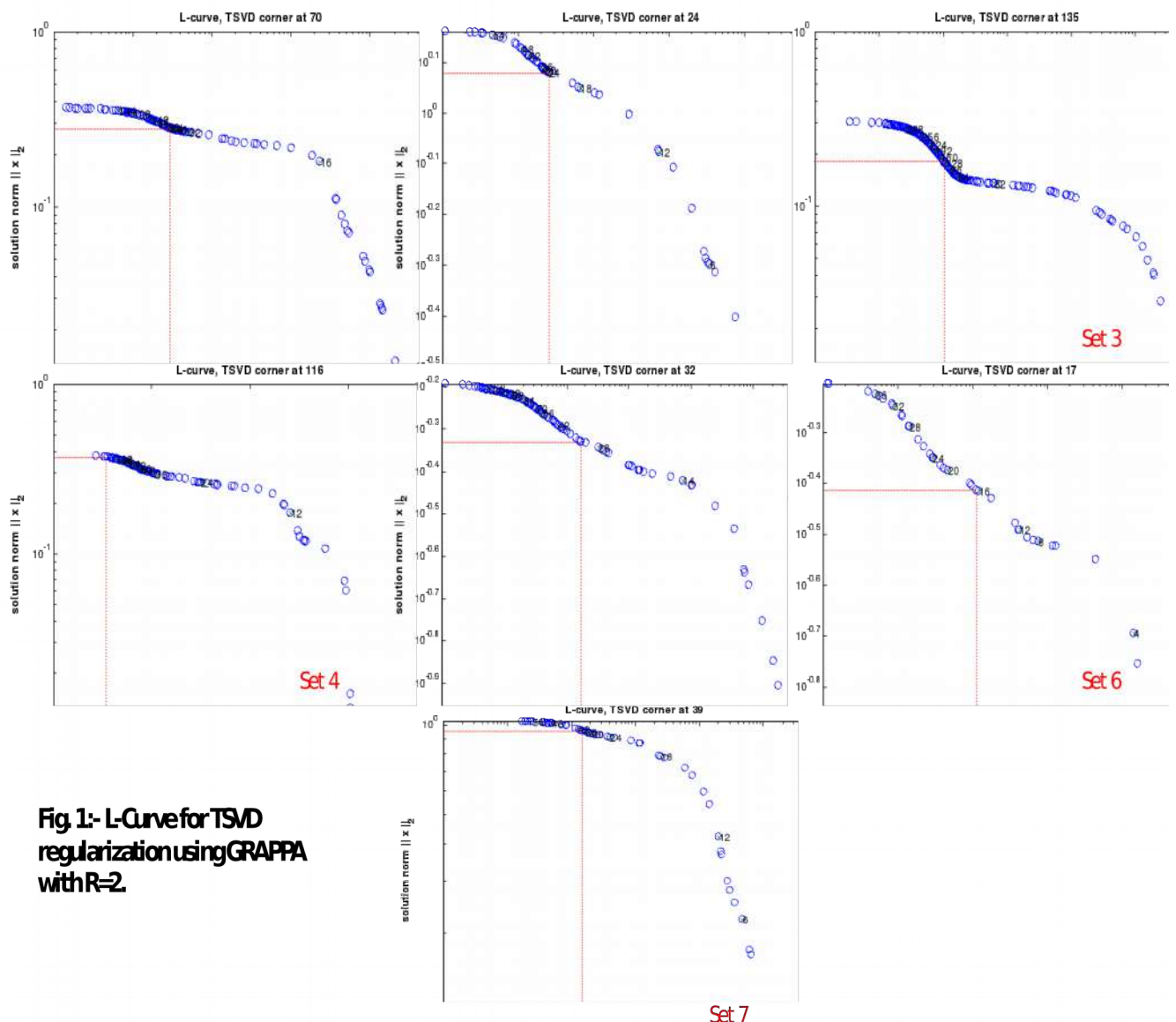


Fig 1- L-Curve for TSVd regularization using GRAPPA with $R=2$.

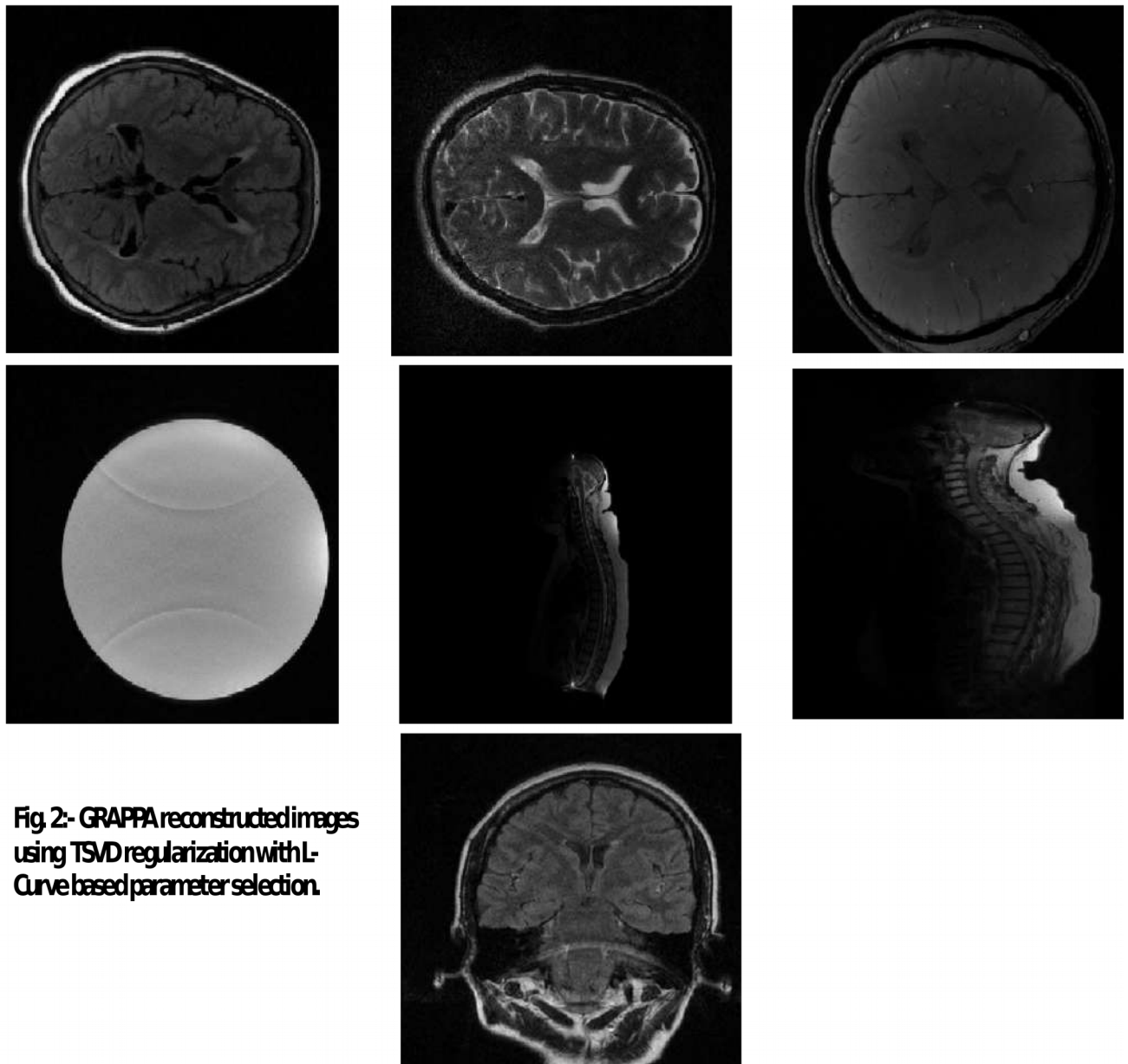


Fig. 2- GRAPPA reconstructed images using TSVD regularization with L-Curve based parameter selection.

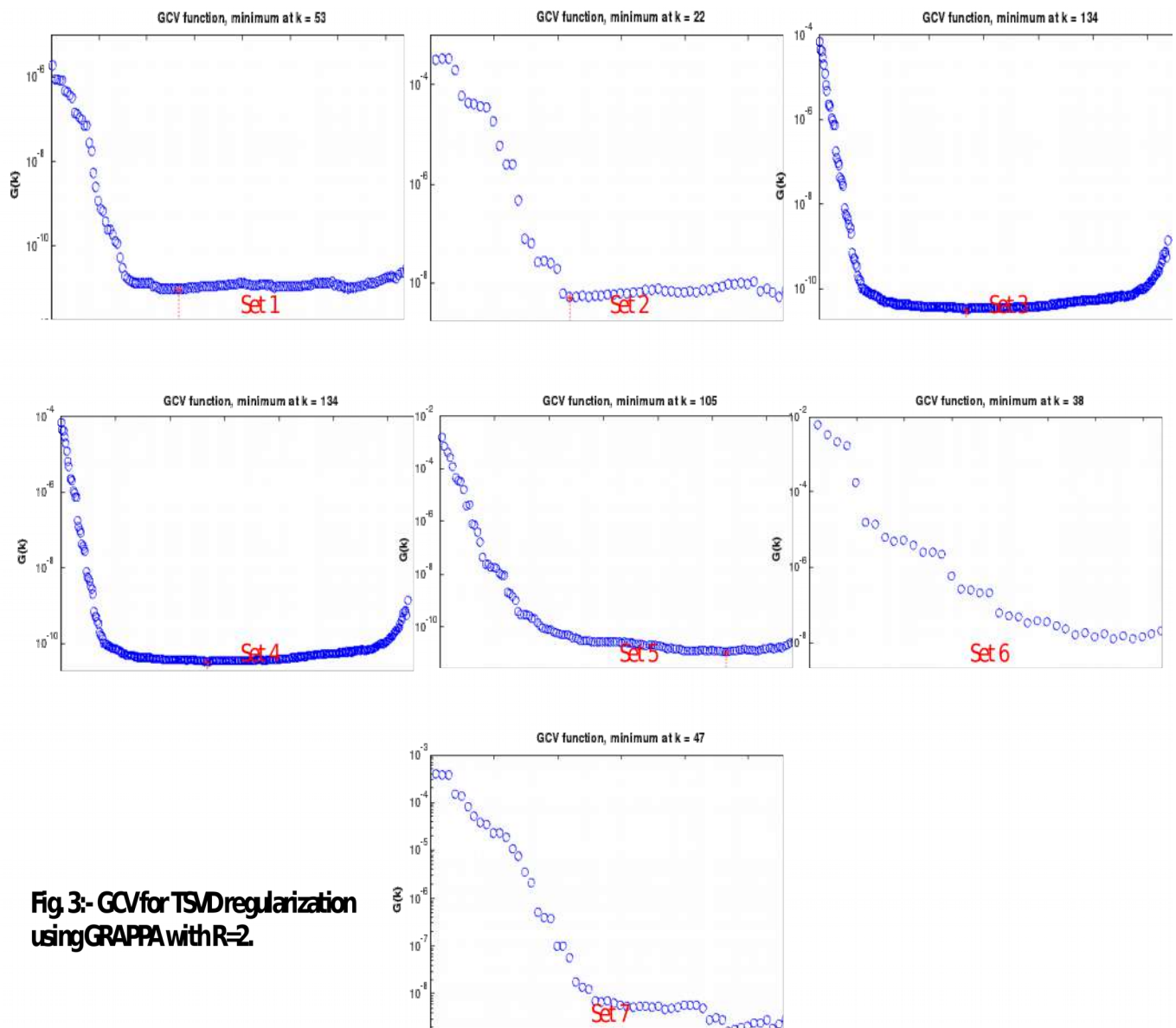


Fig.3:- GCV for TSM regularization using GRAPPA with R=2.

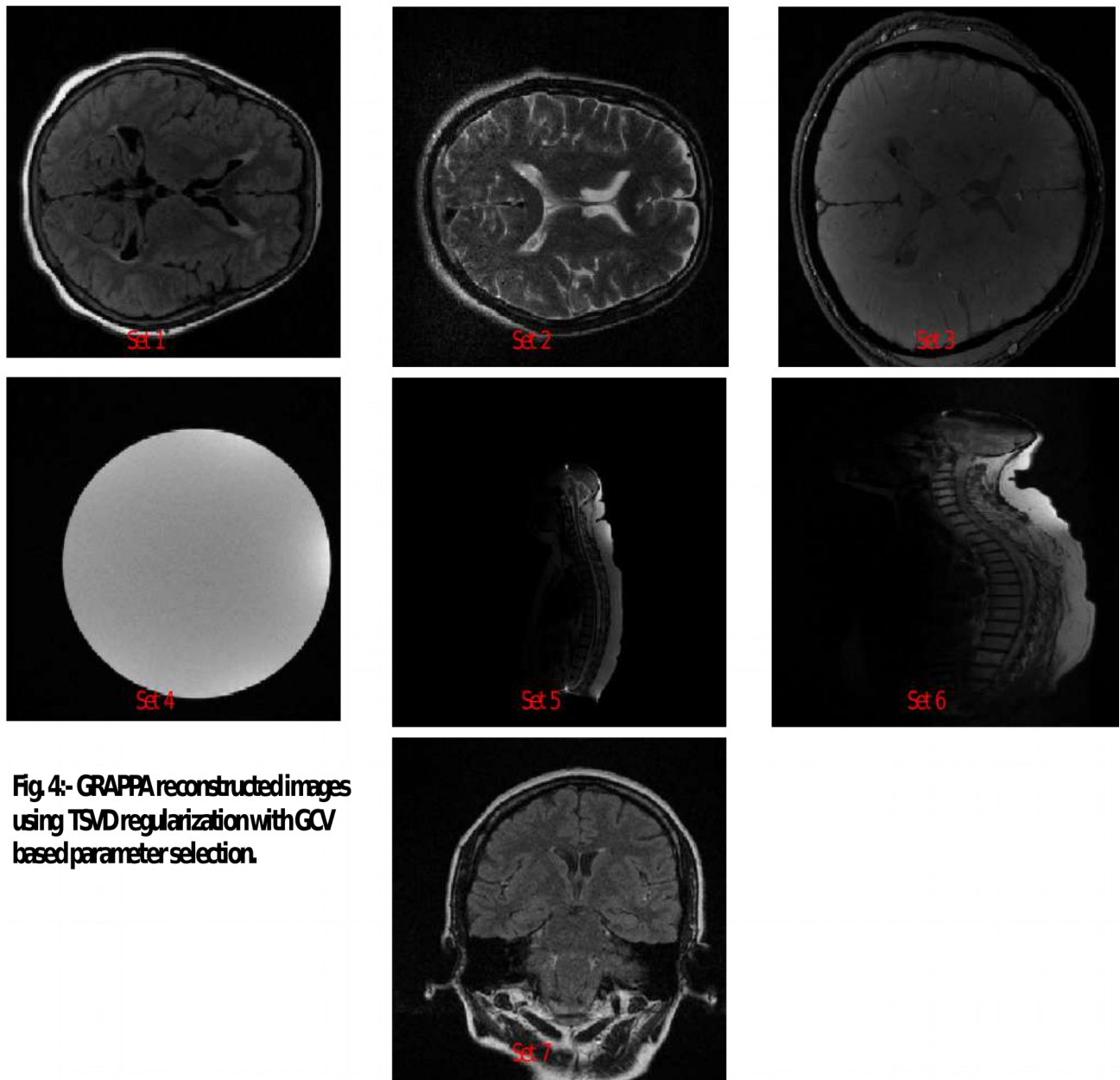


Fig.4:- GRAPPA reconstructed images using TSVd regularization with GCV based parameter selection.

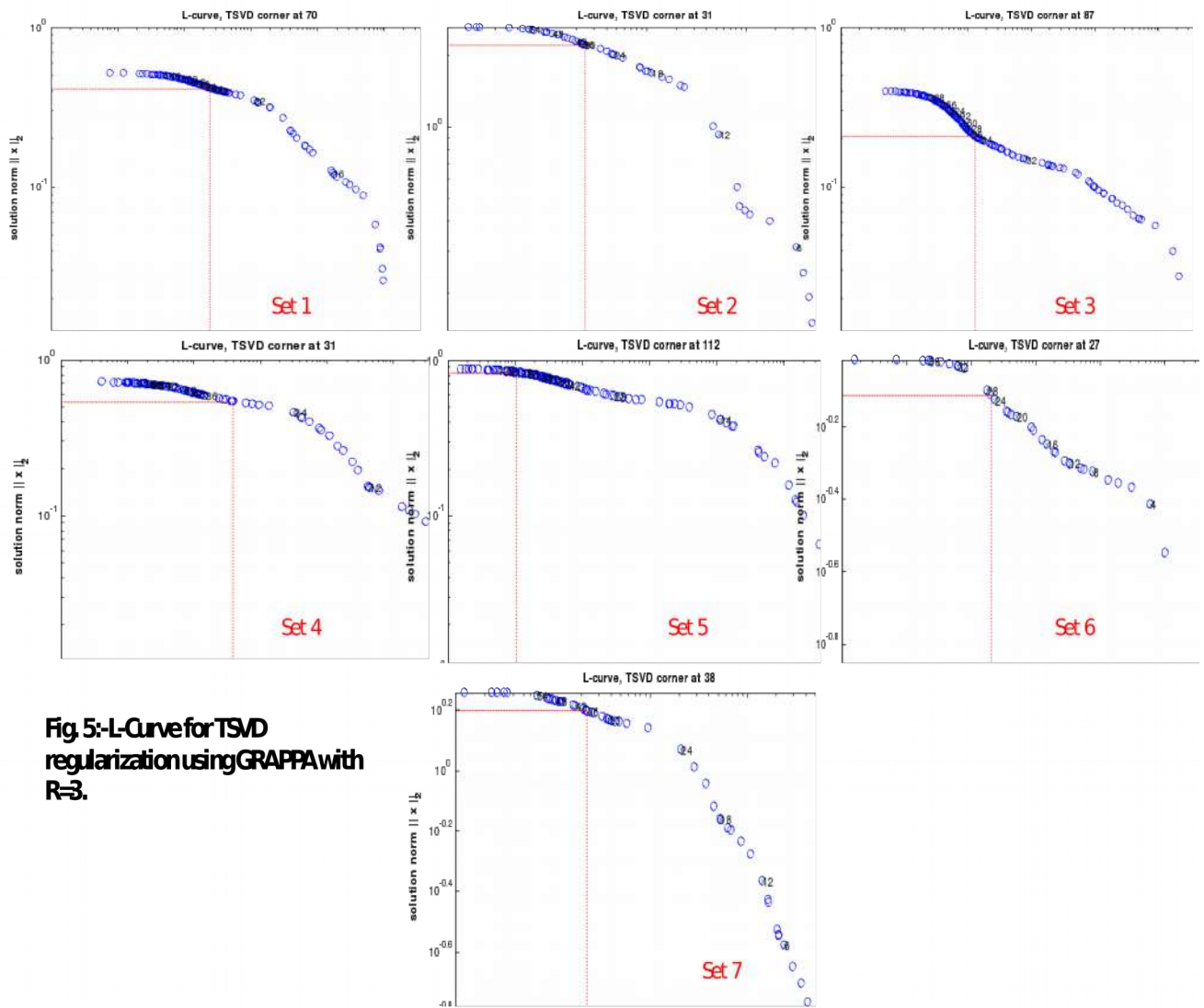


Fig.5:L-Curve for TSVd regularization using GRAPPA with R=3.

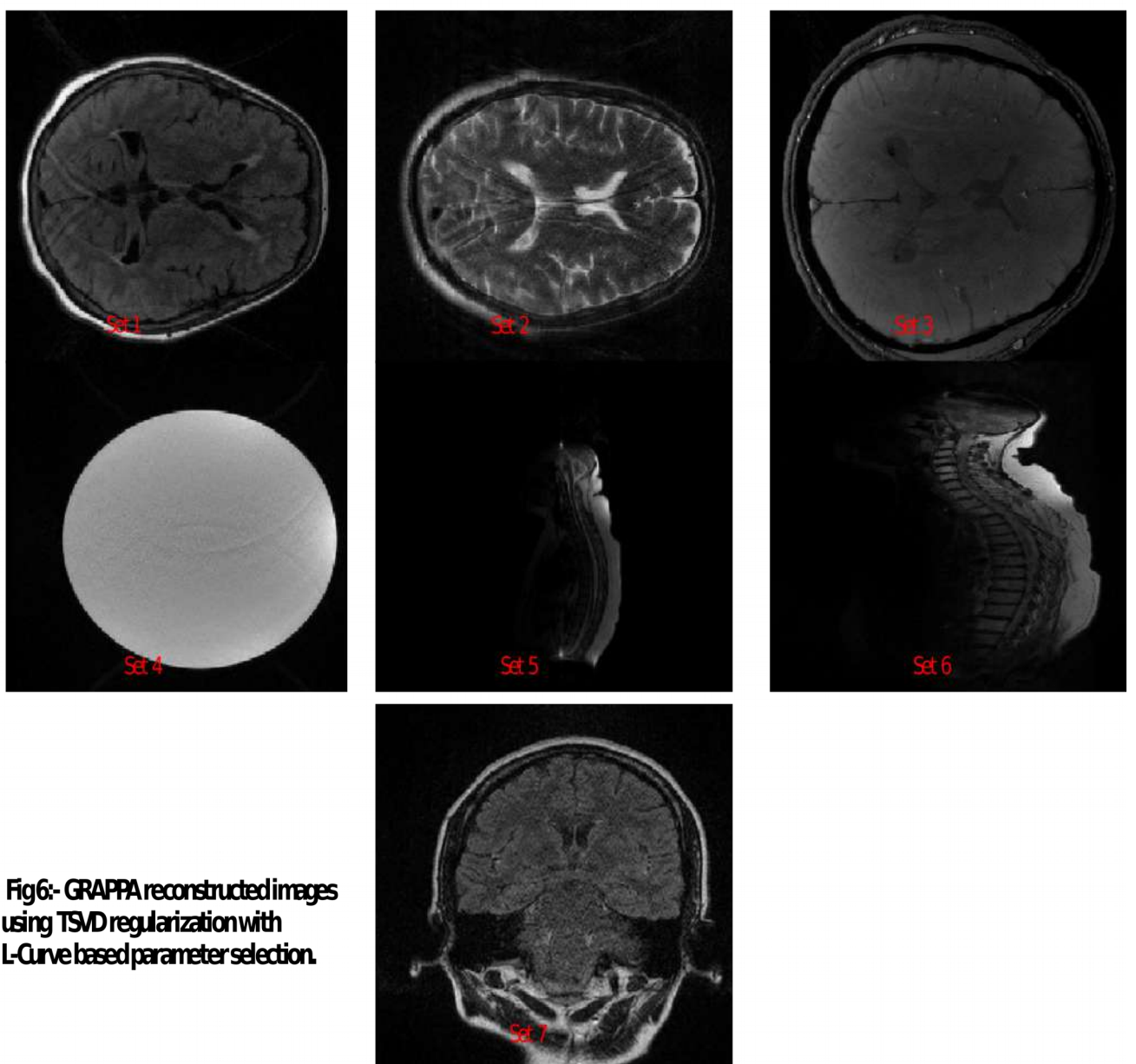


Fig6:- GRAPPA reconstructed images using TSVD regularization with L-Curve based parameter selection.

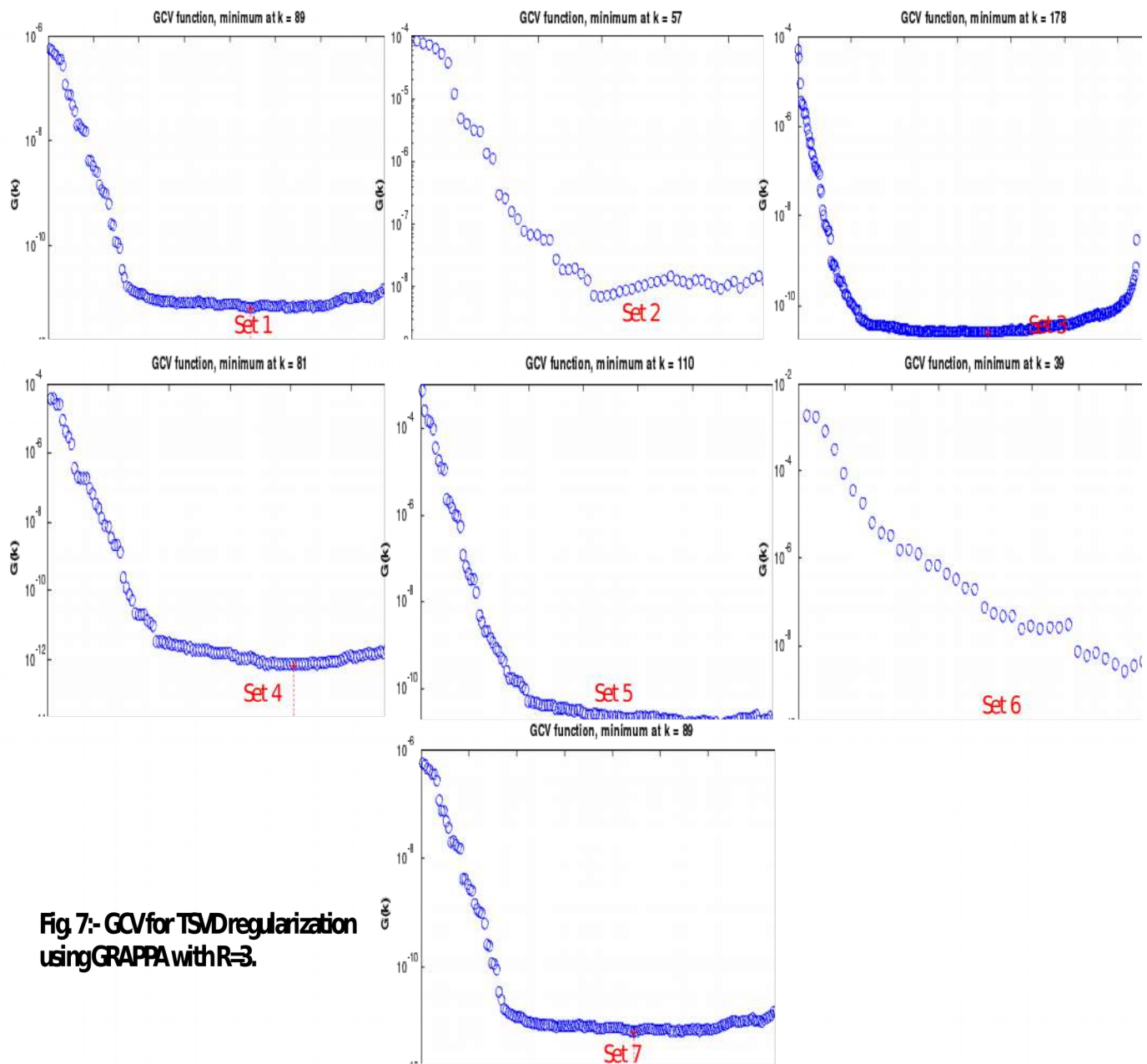


Fig.7:- GCV for TSM regularization using GRAPPA with R=3.

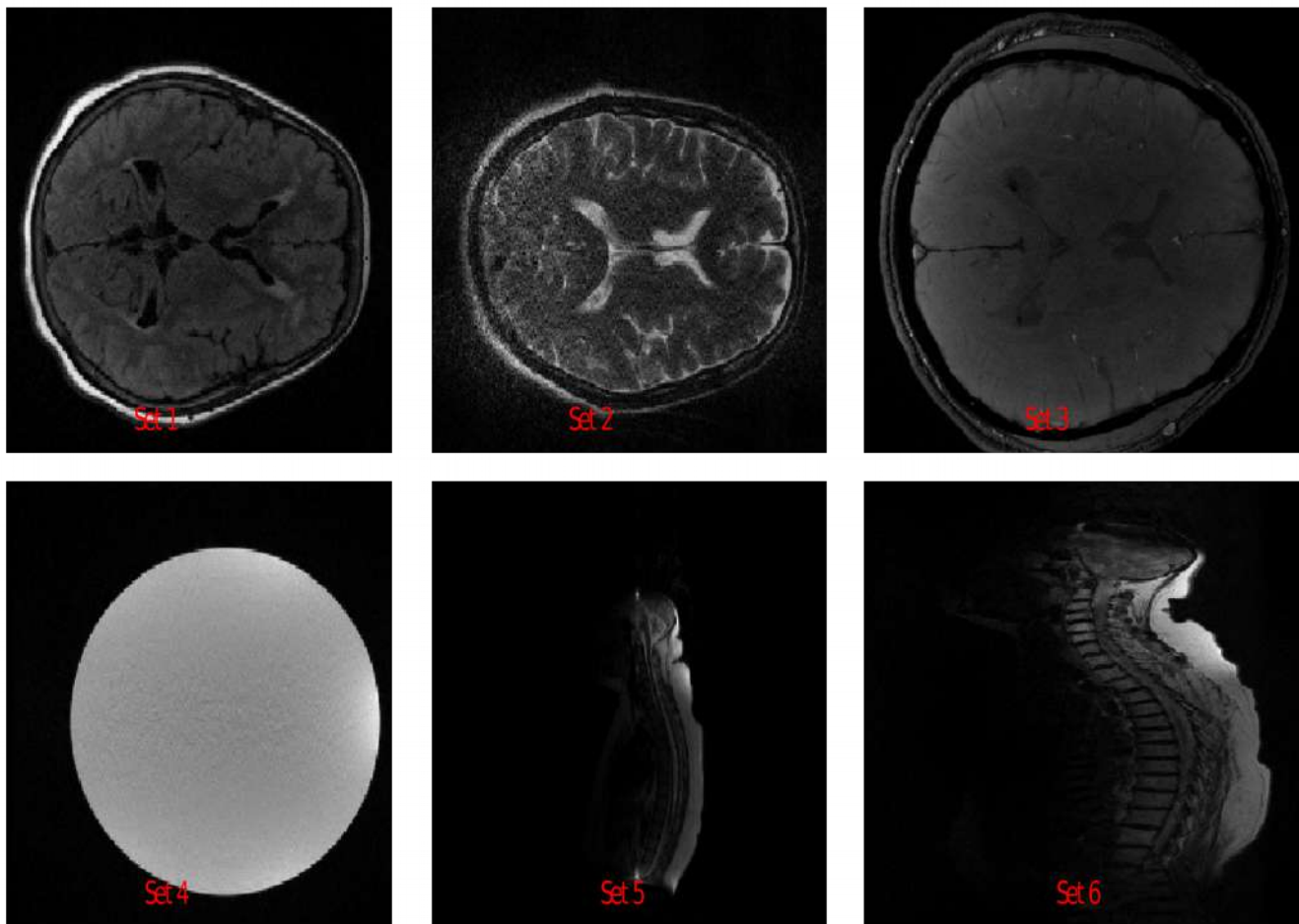
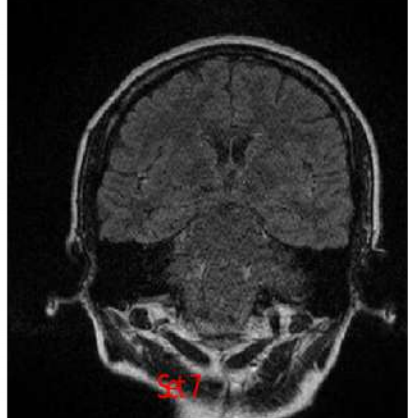


Fig8:- GRAPPA reconstructed images using TSV regularization with GCV based parameter selection.



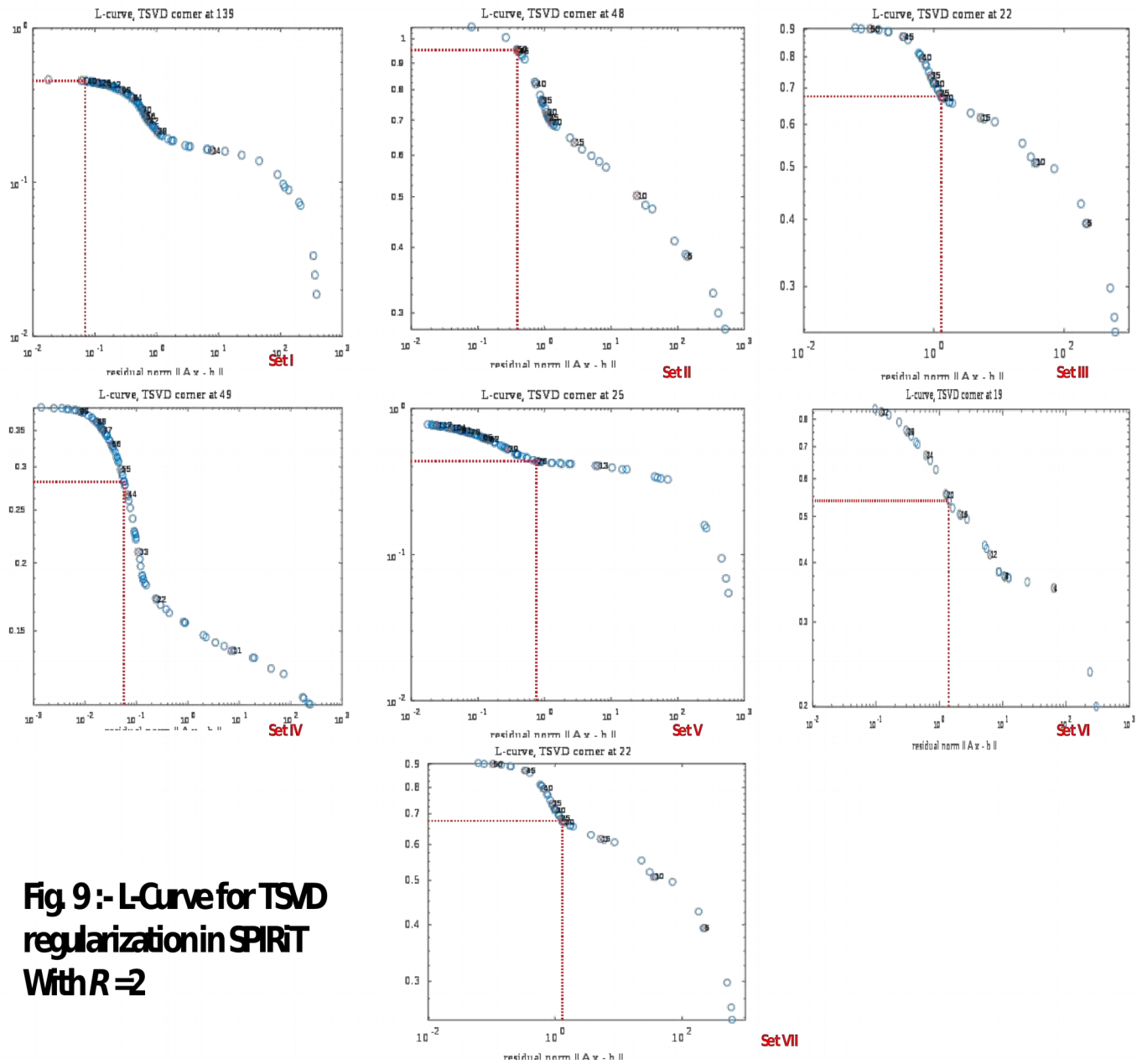
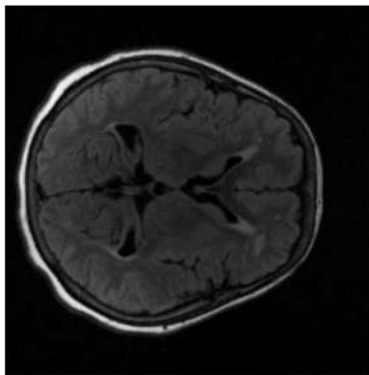
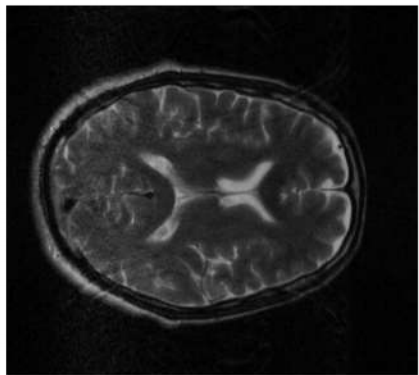


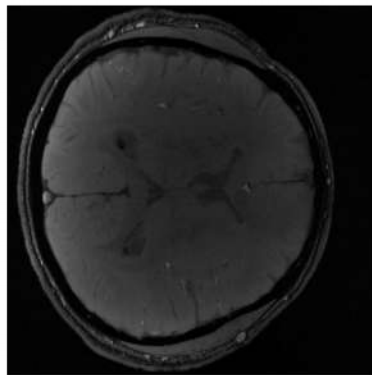
Fig. 9 :- L-Curve for TSVd regularization in SPIRiT With $R=2$



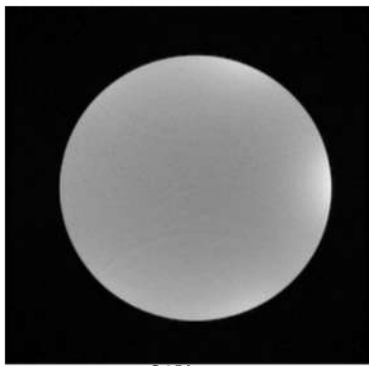
Set I



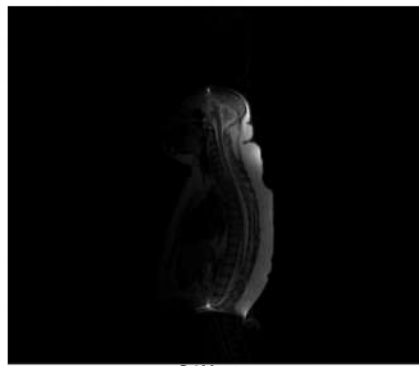
Set II



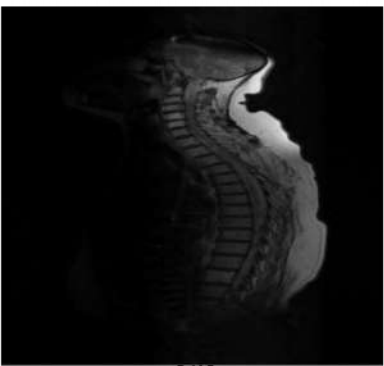
Set III



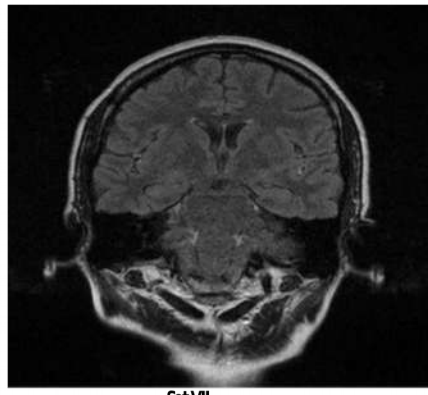
Set IV



Set V



Set VI



Set VII

**Fig. 10:- SPIRIT
reconstructed images using
TSVD regularization with L-
curve based parameter
selection**

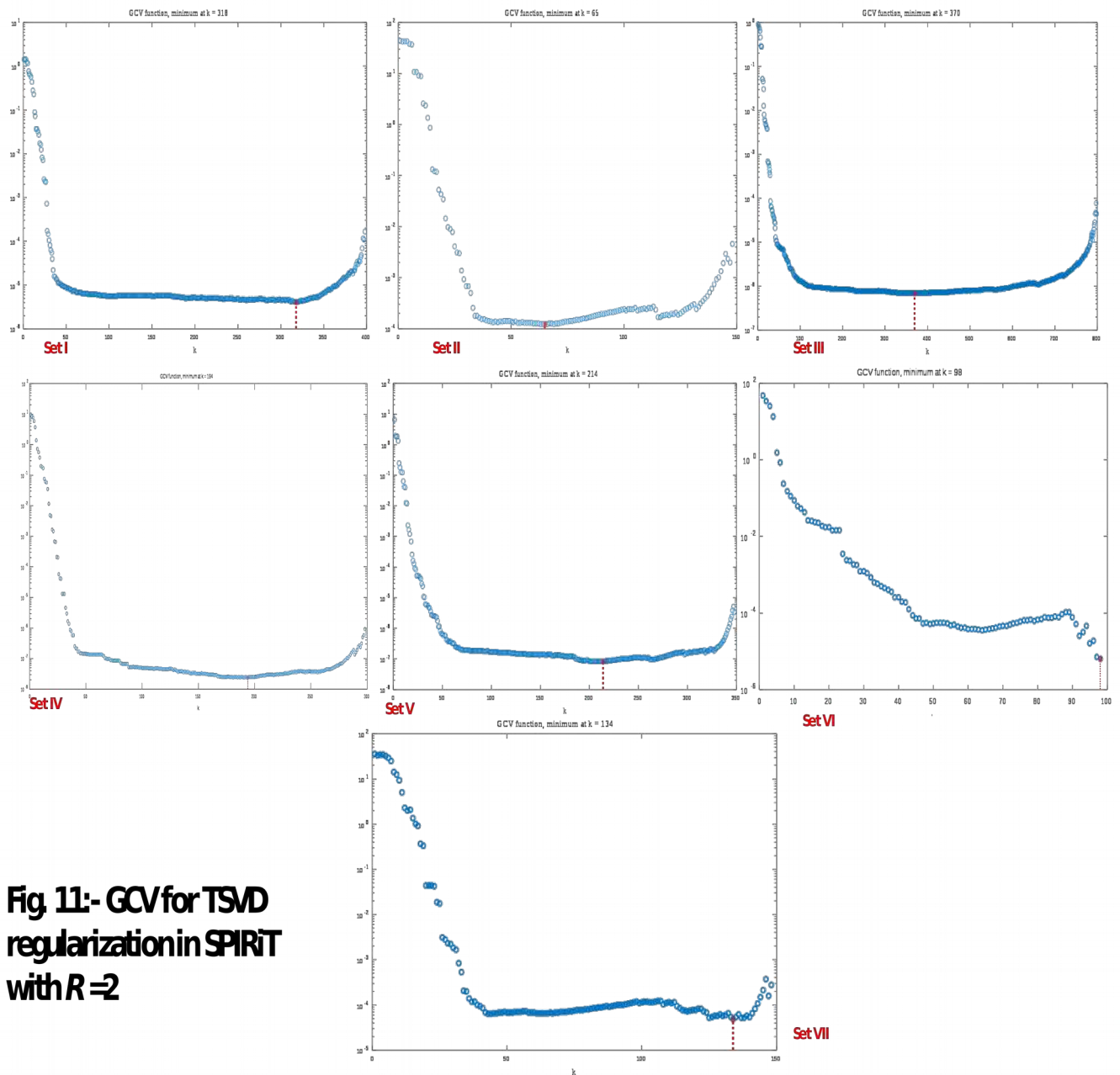
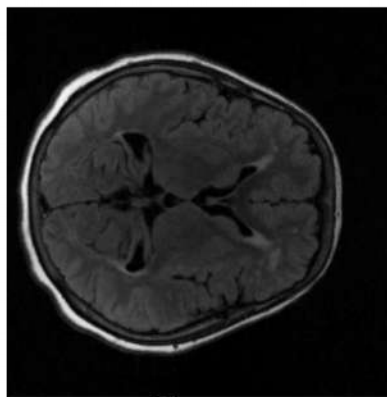
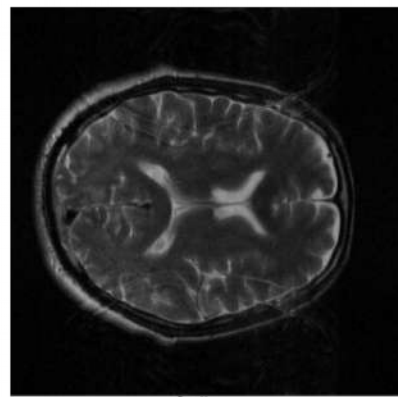


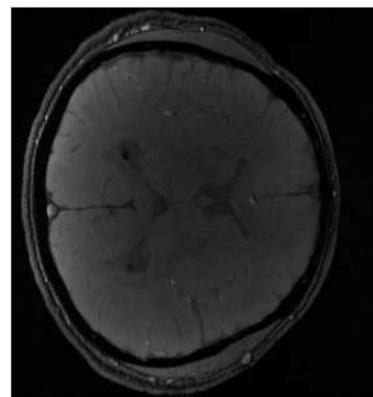
Fig. 11:- GCVfor TSVd regularization in SPIRiT with $R=2$



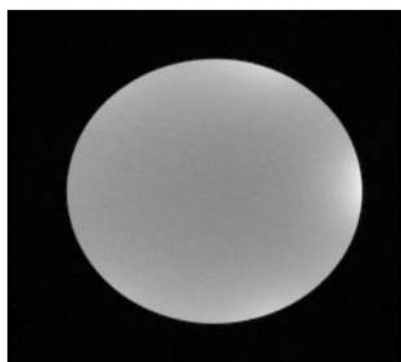
Set I



Set II



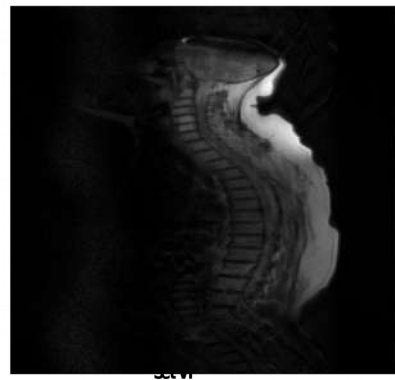
Set III



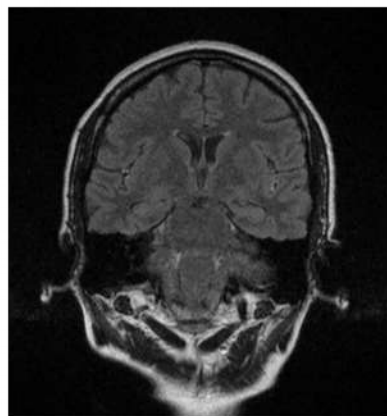
Set IV



Set V



Set VI



Set VII

Fig 12:- SPIRiT reconstructed images using TSVD regularization with GCV based parameter selection

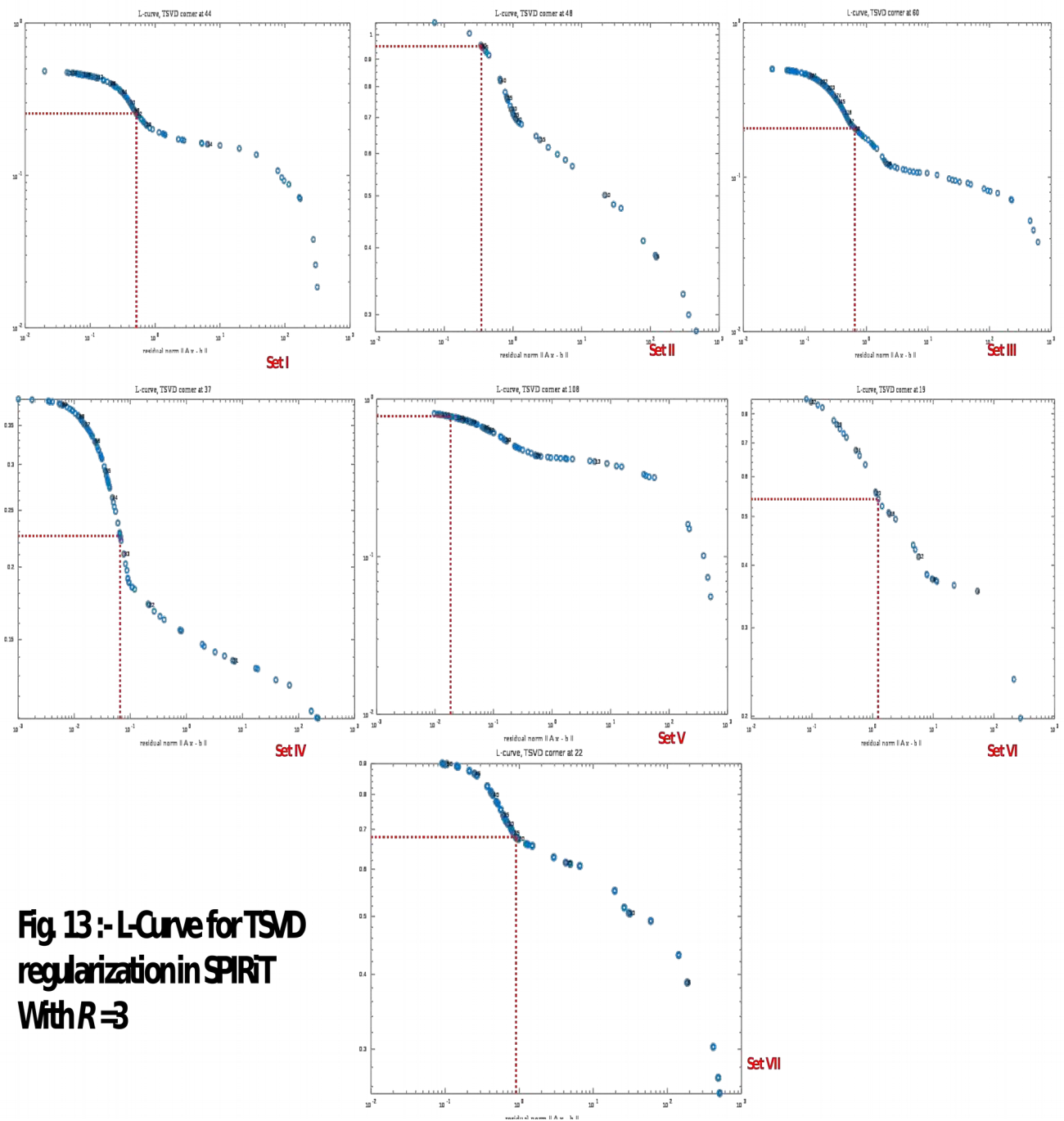
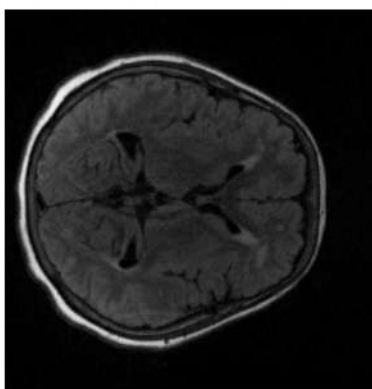
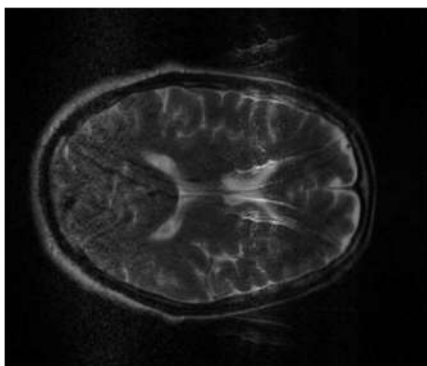


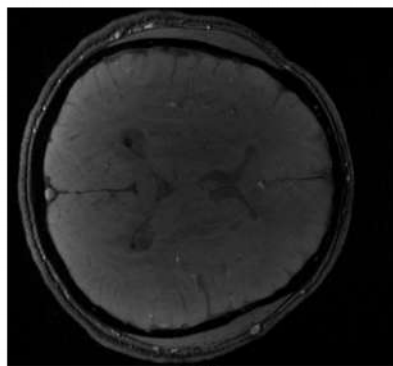
Fig 13 : L-Curve for TSVd regularization in SPIRiT With $R=3$



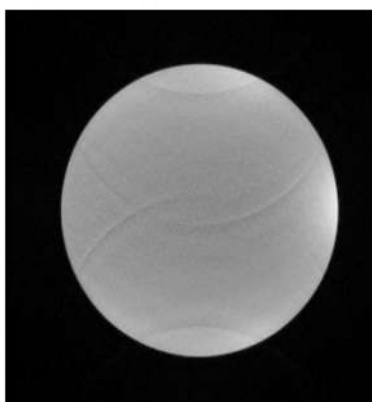
Set I



Set II



Set III



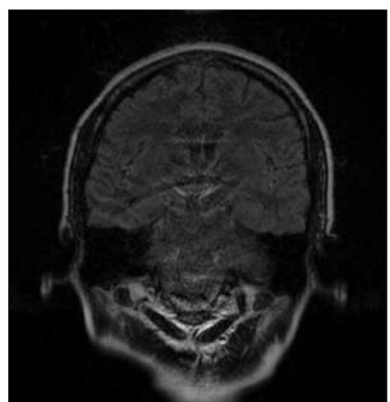
Set IV



Set V



Set VI



Set VII

**Fig. 14:- SPIRIT
reconstructed images using
TSVD regularization with L-
curve based parameter
selection**

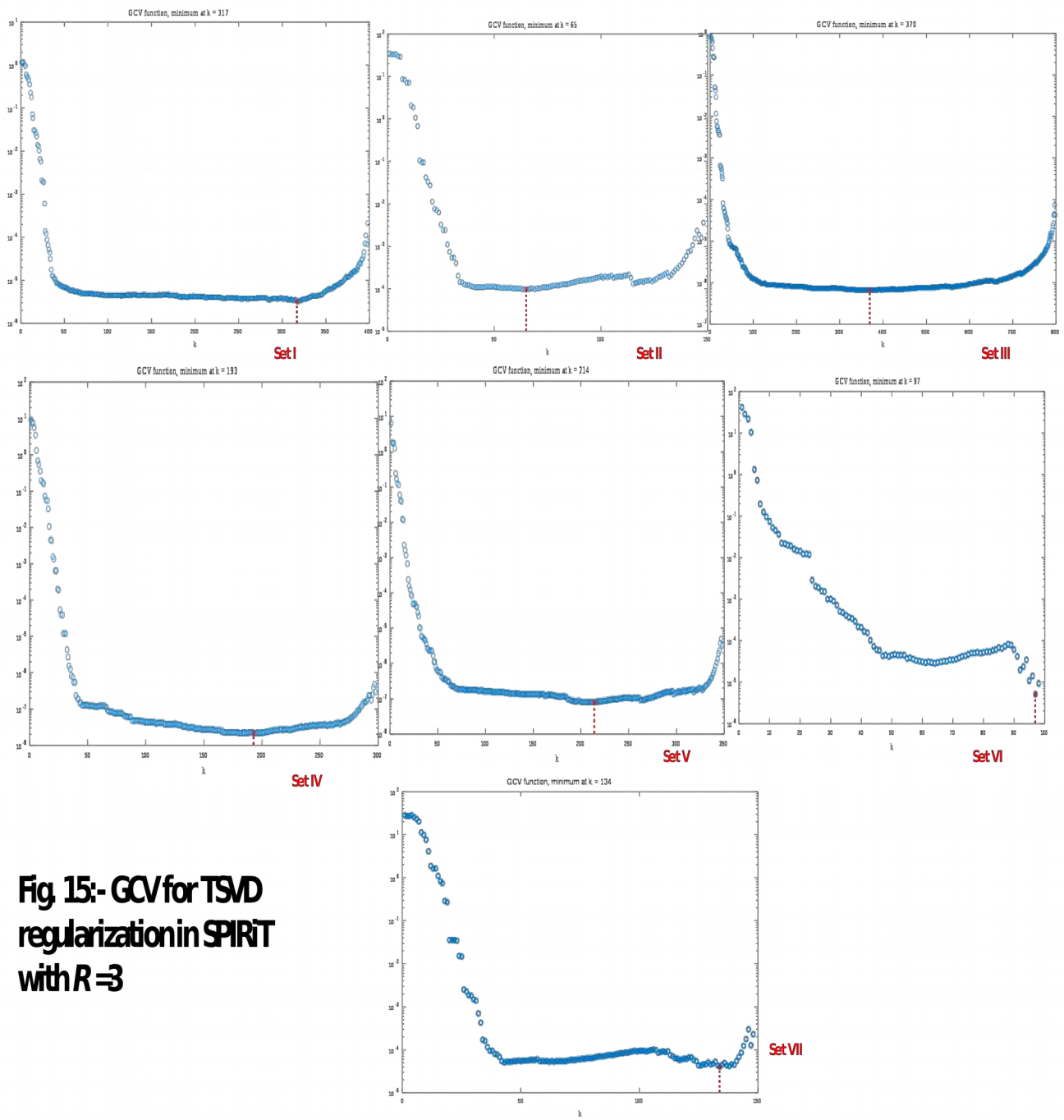


Fig. 15:- GCV for TSVR regularization in SPIRT with $R=3$

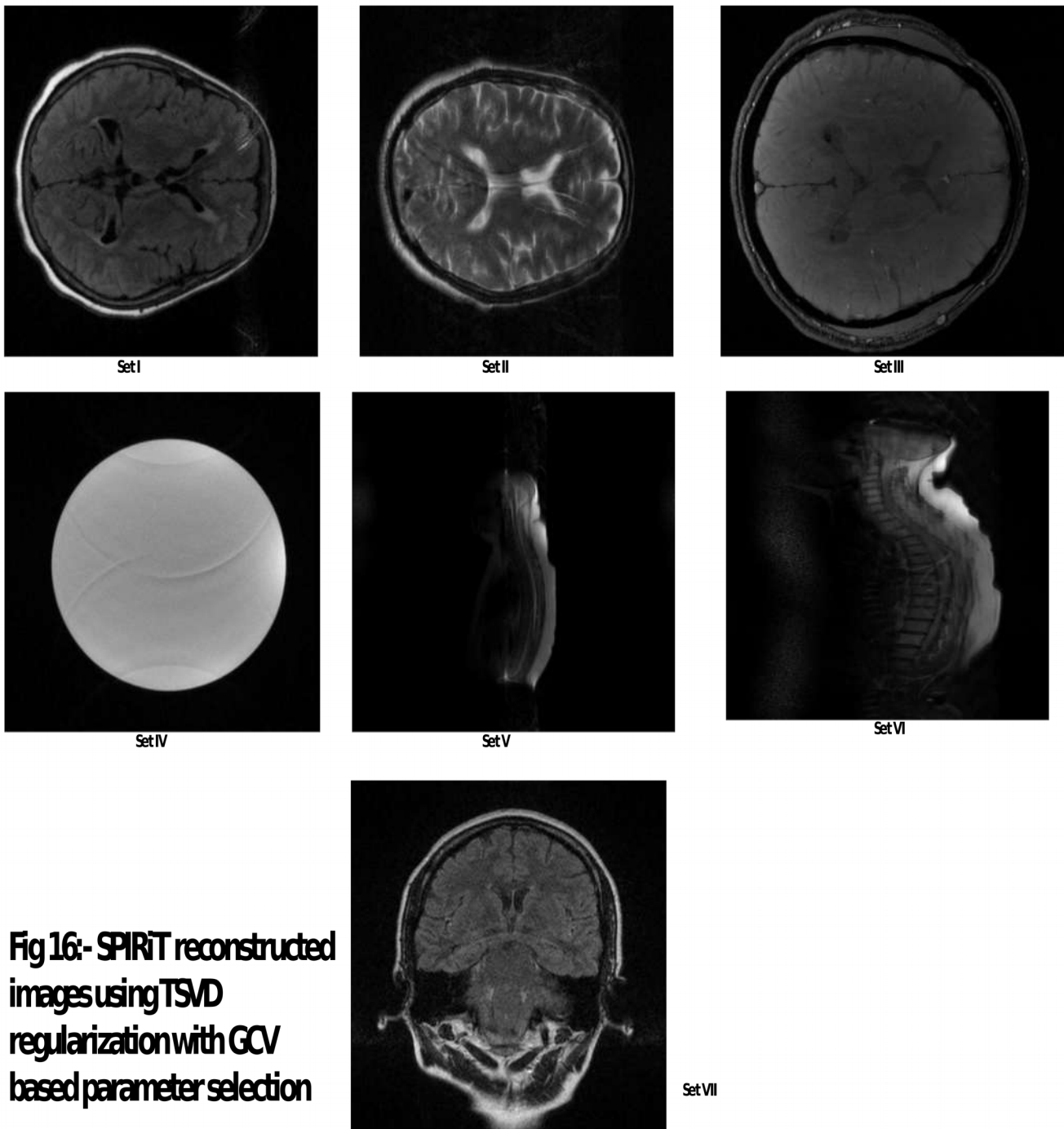


Fig 16:- SPIRiT reconstructed images using TSVD regularization with GCV based parameter selection

Table 1:- Description of datasets I to VII

Data Set	Pulse Sequence	Coil Type	nACS
I	FLAIR_v17	16-channel head array	32
II	T ₂ weighted spin echo	6-channel head array	32
III	SWI gradient echo	32-channel head array	24
IV	T ₂ weighted spin echo	12-channel head array	24
V	T ₂ weighted spin echo	14-channel head array	18
VI	T ₂ weighted spin echo	4-channel head array	26
VII	FLAIR	6-channel head array	26

Table 2:- Reconstruction error of GRAPPA reconstructed images using TSVD regularization method

Dataset	I	II	III	IV	V	VI	VII
L-curve with R=2	0.1902	0.0649	0.0505	0.0604	0.1521	0.0739	0.0608
GCV with R=2	0.1902	0.0644	0.0505	0.0629	0.1547	0.0743	0.0517
L-curve with R=3	0.1768	0.0840	0.0555	0.0625	0.1250	0.0812	0.0583
GCV with R=3	0.1876	0.1329	0.0566	0.0627	0.1250	0.0836	0.0583

Table 3:- Reconstruction error of SPIRiT reconstructed images using TSVD regularization method

Data set	I	II	III	IV	V	VI	VII
L-curve ($R=2$)	0.04765	0.1367	0.07339	0.02068	0.08843	0.0612	0.07349
L-curve ($R=3$)	0.08548	0.1736	0.07823	0.03453	0.1045	0.0929	0.1306
GCV ($R=2$)	0.0463	0.1216	0.03276	0.02063	0.1052	0.1196	0.06541
GCV ($R=3$)	0.0845	0.1586	0.07545	0.03454	0.1815	0.1583	0.1035

**Table 4:- Parameters of cross-over determination in
GRAPPA calibration for datasets I to VII with R=2**

Data Set	Pulse Sequence	nACS	M	σ_k^0	σ_{\min}^0	$\sigma^0 \times 10^5$	T _v	v
I	FLAIR_v17	32	4096	0.0448	0.0223	4.46	15	1.01
II	T2 weighted spin echo	32	5120	0.3572	0.0357	7.14	34	3.50
III	SWI gradient echo	24	2240	0.0660	0.0279	5.58	16	1.01
IV	T2 weighted spin echo	24	3456	0.0481	0.0118	2.336	12	1.02
V	T2 weighted spin echo	18	6144	0.0933	0.0020	0.40	21	2.10
VI	T2 weighted spin echo	26	5376	0.1108	0.0372	7.44	14	2.00
VII	FLAIR	26	4992	0.2356	0.0461	9.22	12	1.52

Table 3:- Parameters of cross-over determination in GRAPPA calibration for datasets I to VII with R=3

Data Set	Pulse Sequence	nACS	M	σ_k^0	σ_{\min}^0	$\sigma \times 10^5$	T _v	v
I	FLAIR_v17	32		0.1049	0.0171	0.3424	3	2.72
II	T2 weighted spin echo	32		0.0307	0.0286	0.5744	4	5.06
III	SWI gradient echo	24		0.0482	0.0475	9.5040	1	0.68
IV	T2 weighted spin echo	24		0.1699	0.00978	0.1995	3	2.60
V	T2 weighted spin echo	18		0.1047	0.0135	0.2720	3	4.15
VI	T2 weighted spin echo	26		0.2049	0.0311	0.6226	3	4.09
VII	FLAIR	26		0.3158	0.0371	0.7428	2	2.29

Table 6:- Parameters of cross-over determination in SPIRiT calibration for datasets I to VII with R=2

Data Set	Pulse Sequence	Coil Type	nACS	M	σ_k^0	σ_{\min}^0	$\sigma^0 \times 10^{-5}$	T _v	v
I	FLAIR_v17	16-channel head array	32		0.0191	0.0011	2.23	15	1.03
II	T ₂ weighted spin echo	6-channel head array	32		0.0283	0.0018	5.00	11	2.28
III	SWI gradient echo	32-channel head array	24		0.0644	0.0038	7.61	8	1.98
IV	T ₂ weighted spin echo	12-channel head array	24		0.0180	0.0003	0.60	42	1.52
V	T ₂ weighted spin echo	14-channel head array	18		0.0212	0.0010	2.00	10	1.50
VI	T ₂ weighted spin echo	4-channel head array	26		0.0268	0.0037	7.40	5	1.02
VII	FLAIR	6-channel head array	26		0.0071	0.0040	8.00	8	1.01

Table 7:- Parameters of cross-over determination in SPIRiT calibration for datasets I to VII with R=3

Data Set	Pulse Sequence	Coil Type	nACS	M	σ_k^0	σ_{\min}^0	$\sigma^0 \times 10^{-5}$	T _v	v
I	FLAIR_v17	16-channel head array	32		0.04137	0.001059	2.118	1	0.6053
II	T ₂ weighted spin echo	6-channel head array	32		0.03694	0.002443	4.886	10	1.9063
III	SWI gradient echo	32-channel head array	24		0.04369	0.002939	5.878	5	1.1776
IV	T ₂ weighted spin echo	12-channel head array	24		0.02129	0.0003254	6.5080	43	2.3205
V	T ₂ weighted spin echo	14-channel head array	18		0.02022	0.0007586	1.5172	13	1.3728
VI	T ₂ weighted spin echo	4-channel head array	26		0.0301	0.003874	7.7480	5	0.8327
VII	FLAIR	6-channel head array	26		0.005554	0.004214	0.008428	41	-0.0033